# Well Trajectory Optimization for SAGD

John G. Manchuk and Clayton V. Deutsch

*Forecasting the potential recoverable bitumen from a SAGD drainage area is dependent on several factors including reservoir geometry, heterogeneity, operating conditions, and well pair position. Implementing good well trajectory design increases the amount of recoverable bitumen and the economic value of the project. Understanding the sensitivity of the design relative to different reservoir and engineering parameters is useful decision support information. Moreover, the optimal positioning of well pairs interacts with the layout of the drainage areas and associated surface pad facilities. This paper develops a well trajectory optimization approach that designs trajectories so that the potential recovery from a well pair is maximized. The approach is designed primarily to support the optimization of drainage area configurations developed in the associated paper; therefore, trajectories are optimized in two dimensional cross sections of the reservoir that run along the well length and along depth or elevation through the reservoir. Optimization is based on surfaces that reflect the quality of the reservoir and include a base surface and net and gross bitumen thickness surfaces. The algorithm can optimize wells that are strictly horizontal, or that are deviated within specified constraints that include limitations on slope of the trajectory and on the elevation offset from the deepest to the shallowest part of a trajectory. The interior point Newton method is used to solve the constrained optimization problem.*

**Introduction**

For unconventional recovery techniques such as SAGD that involve horizontal wells, well design becomes an important issue for maximizing the recovery potential. Geology of heavy oil deposits such as the McMurray formation is heterogeneous (Ranger and Gingras, 2003; Deutsch, 2010): surfaces that describe the base and top of a recoverable zone could be quite rough or irregular and the spatial distributions of reservoir properties such as porosity, permeability, and bitumen saturation show significant variations. Moreover, the presence of other features such as bottom water and thief zones (Pooladi-Darvish and Matter, 2002; Doan et al, 2003; Law et al, 2003) introduces additional recovery risks that could lead to poor well performance if they are not taken into consideration. Uncertainty is another source of recovery risk that should be considered for well design. The geological features and petrophysical properties of the reservoir are never known for certain. Uncertainty is accounted for by generating a set of alternate realities or realizations to represent possible truths. Uncertainty should be incorporated into well design by considering all realizations. Designing wells with one realization should be avoided. There is a risk that the chosen realization does not represent the true reservoir everywhere. Also, considering only one realization would lead to a design suited to that realization, but not the other possibilities; thus, the predictions would be too optimistic.

In this work, well design refers to determining the optimal depth and trajectory of a generally horizontal production well in a SAGD drainage area (DA). Different approaches can be used to solve this problem. For example, detailed 3D reservoir models and flow simulation could be used to test the performance of a design; however, this can be a very time consuming process. Simplifications are made in this approach so that good designs may still be obtained in a fraction of the time. For purposes of optimizing DA configurations (Manchuk and Deutsch, 2012), the model is simplified to 2D, being represented by surfaces rather than volumes. Well trajectories can be designed very fast in this case, which is advantageous for the DA optimization problem.

A description of the well design problem and related functions for approximating potential recovery are provided in the first section of this paper. Well trajectory design is a constrained optimization problem that is solved using the interior point Newton method and is developed in section 2. The objective function for optimization is to minimize the potential loss in recovery, which is measured as the volume of bitumen left behind for a given well design. Testing is done on a few examples in section 3 for one reservoir model and for stochastic cases where multiple realizations are accounted for.

## Problem Description

The optimization problem is to determine the optimal depth and trajectory of a production well in a SAGD drainage area (DA) with the objective of minimizing potential loss in recovery . Due to computational complexity and time constraints, loss is evaluated based on a set of surfaces that describe the geometry and quality of the producible zone, where quality is a measure of the bitumen in place. Three variables that describe the reservoir are required and include a reservoir quality variable, a base surface, and gross thickness. In this work, reservoir quality is summarized using net continuous bitumen (NCB) that is the total thickness of recoverable bitumen above the base surface (Figure 1). Net reservoir is often determined based on facies and cut-offs for porosity, permeability and water saturation. The base surface is a base of continuous bitumen (BCB) that defines the lowest elevation a horizontal well could retain while still being able to recover bitumen from above. The BCB, NCB and GCB surfaces are derived from a 3D reservoir model. They can be deterministic if only a single reservoir model is available or stochastic if the reservoir is modeled by a set of realizations. In the latter case, the optimization problem is solved in a probabilistic sense, accounting for the uncertainty that is quantified by the set of realizations.

The objective function for optimizing well trajectories is defined in barrels of bitumen and provides a measure of the potential volume a production well could recover based on information from the 2D surfaces. This volume is actually evaluated as an area from a vertical cross section that traverses the well (Figure 2) along coordinate $u$ with elevation denoted $z$. The well trajectory is defined as $z(u)$, or elevation as a function of $u$. The point $u = 0$ indicates the start of the producible portion of a well, or the heel, and $u = 1$ indicates the end of the producible portion, or the toe.

Well trajectory elevation is not restricted to be horizontal. Some flexibility within user specified constraints is permitted so that trajectories may be designed to provide better conformance to the BCB surface than a strictly horizontal well. To allow flexibility, wells are represented using a Hermite spline (Hearn and Baker, 2004), which is a piecewise cubic polynomial defined by Eq. 1, where $a, b, c, d$ are constants.

$$z(u) = au^3 + bu^2 + cu + d \tag{1}$$

Hermite splines are defined by four parameters: two end-points and the slope at each end-point. For a well, the endpoints are at $(u, z(u)), u = 0,1$, and the slopes are defined by $z'(u), u = 0,1$, where $z'(u)$ is defined by Eq. 2.

$$z'(u) = 3au^2 + 2bu + c \tag{2}$$

Knowing the endpoints and slopes, the elevation of any point along a trajectory is defined by Eq. 3, where **M** is a Hermite coefficient matrix.

$$\begin{aligned} z(u) &= \mathbf{uMc} \\ &= \begin{bmatrix} u^3 & u^2 & u & 1 \end{bmatrix} \begin{bmatrix} 2 & -2 & 1 & 1 \\ -3 & 3 & -2 & 1 \\ 0 & 0 & 1 & 0 \\ 1 & 0 & 0 & 0 \end{bmatrix} \begin{bmatrix} z(0) \\ z(1) \\ z'(0) \\ z'(1) \end{bmatrix} \end{aligned} \tag{3}$$

Hermite splines have nice features for well trajectory specification. With only two endpoints, the well cannot have more than one undulation (up-down-up feature or vice versa). Having more undulations could be detrimental to production since such a design has a tendency to impede flow. Since the endpoints and slopes are specified, it is possible to consider wells that are strictly horizontal or strictly linear with a constant slope. Wells can be defined as toe-up or toe-down (Figure 3). Incorporating constraints such as a maximum slope and maximum allowable vertical deviation along the well is possible (Figure 4), where maximum vertical deviation measures the elevation difference between the highest and lowest points along a trajectory.

Maximum vertical deviation and maximum allowable slope constraints have been incorporated into the well trajectory optimization problem. These constraints are important because they could relate to production performance. For example, too excessive of a slope may lead to ineffective pressure and thermal gradients along the producer that could impede flow. Too large a vertical deviation along a well could also lead to a portion of a producer being close to or above the elevation of the associated injector (Figure 5). This situation could lead to premature steam bypass from the injector into the producer. If the elevation offset from the producer to the injector is to be 5 m for example, the maximum vertical deviation should be no more than 5 m. Further explanation is provided on these constraints in the following section on optimization strategy.

A similar situation where steam bypass can occur is from a neighbouring injector if a production well is too high above it (Figure 6). An additional constraint would need to be incorporated to prevent this situation from occurring. Well trajectories would need to be optimized in a joint fashion for all wells within a drainage area. There may also be a need to consider adjacent DA's when the well pairs are close enough together.

Once a well trajectory is designed, evaluating the area of bitumen lost is done by integration. Although the BCB and other surfaces have been portrayed as continuous thus far, it is more common to encounter these properties as discrete functions that are defined only at the centre of a set of grid cells from a reservoir model (Deutsch, 2002). To facilitate the integration process, discrete functions defining the surfaces are re-parameterized as piecewise linear functions along $u$. The integral is evaluated between the producer and the BCB when $z(u) > z_{BCB}(u)$ and is done using integration by parts, where each part is a segment of the piecewise functions (Figure 7).

The bitumen lost is a function of the well trajectory and the surfaces defined by Eq. 4, which can be interpreted as the portion of NCB below $z(u)$. This assumes the NCB is uniformly distributed between the BCB and TCB and is a consequence of representing 3D models with 2D surfaces. It is possible to utilize other surfaces, for example, one that describes vertical trend information for NCB to give an improved approximation of the true vertical distribution of NCB. Such surface are not explored in this work, but are considered for future research.

$$f(u) = \left( \frac{z(u) - z_{BCB}(u)}{h_{GCB}(u)} \right) h_{NCB}(u) \tag{4}$$

Integrating Eq. 4 for one part is given by Eq. 5, where $u = ak$ and $u = bk$ define the limits of integration for part $k$ and $F_k$ defines the bitumen lost for part $k$.

$$F_k = \int_{ak}^{bk} \left( \frac{z(u) - z_{BCB}(u)}{h_{GCB}(u)} \right) h_{NCB}(u) du \tag{5}$$

The sum of bitumen lost over all parts gives the total bitumen lost; however, not all portions of a producer are necessarily above the BCB. Any portion of the well that is below the BCB is referred to as ineffective well length in this work. In general, ineffective well length leads to additional losses in recoverable bitumen. Because injected steam propagates laterally as well as vertically (Butler, 1991; Butler, 1994), there is some tendency for bitumen to be drained from above ineffective segments into nearby effective portions of the producer. After operating the injector-producer well pair for some time, the steam-oil interface where the majority of drainage occurs can be approximated by a plane with an angle $\theta$ from horizontal (Figure 8). This angle is a user specified value that defines a cone of trapped oil above ineffective well length.

Evaluating bitumen lost for portions of a well that are ineffective involves finding the points of intersection between the producer and the BCB, so that the cones of lost bitumen can be defined. Finding intersections can be done using any root finding technique for continuous polynomials (McNamee, 2007). Halley's method (Scavo and Thoo, 1995) was used in this work. Bitumen lost for a part above ineffective well length is defined by Eq. 6, where $s(u)$ defines the steam-oil interface.

$$F_k = \int_{ak}^{bk} \left( \frac{s(u) - z_{BCB}(u)}{h_{GCB}(u)} \right) h_{NCB}(u) du \tag{6}$$

The limits of integration, $ak$ and $bk$, may take on different values of $u$ depending on how the integration part is defined and include an intersection point, one of the discrete locations, or the apex of the cone. Similarly in Eq. 5, limits of integration may be associated with discrete locations or intersection points.

Selection of $\theta$ can have a significant impact on trajectory design. The extreme cases are zero degrees, which implies that all bitumen above ineffective segments is drained, and 90 degrees, which implies that all bitumen above ineffective segments is lost. A zero degree case is only reasonable if the ineffective segment is short relative to the total length of the well. For longer ineffective well segments, a reasonable value for $\theta$ would be determined by an economically sustainable flow rate because as $\theta$ decreases, so does the flow rate (Butler, 1994).

## Optimization Strategy

The objective function that measures the amount of bitumen lost for a given well trajectory is continuous and twice differentiable so it is possible to parameterize the optimization problem using Newton's method (Boyd and Vandenberghe, 2004; Sun and Yuan, 2006). The optimization problem is to minimize the total bitumen lost over the length of a production well. Total bitumen lost is defined by Eq. 7, where $m$ is the total number of parts for integration and $L$ is the number of realizations if the problem is stochastic.

$$\begin{aligned} F &= \sum_{l=1}^{L} \sum_{k=1}^{m} \int_{ak}^{bk} \left( \frac{t(u) - z_{BCB,l}(u)}{h_{GCB,l}(u)} \right) h_{NCB,l}(u) du \\ t(u) &= \begin{cases} z(u) & z(u) \geq z_{BCB,l}(u) \\ s(u) & z(u) < z_{BCB,l}(u) \end{cases} \end{aligned} \tag{7}$$

In deterministic cases, $L = 1$, and the outer sum is not necessary. For multiple realizations, this Eq. gives total bitumen lost over all realizations, as opposed to the mean loss, since either case will result in the same optimal trajectory. However, it is not correct to optimize the trajectory with the mean of the BCB, GCB and NCB surfaces as this approach is not guaranteed to minimize the mean loss over all realizations due to the non-linear objective function.

Newton's method requires the gradient, $\nabla F$, and Hessian, $\nabla^2 F$, of the objective function that is determined by evaluating the integral in terms of $u$ and taking the first and second derivative in terms of the parameters in the vector $\mathbf{c}$ from Eq. 3. This information is adequate to solve the unconstrained well trajectory optimization problem, where $\mathbf{c}$ is updated iteratively according to Eq. 8, and $\alpha$ is the step size usually determined using a line search to prevent divergence. The approach is summarized in Algorithm 1.

$$\mathbf{c}_j = \mathbf{c}_{j-1} + \alpha \left( \nabla^2 F \right)^{-1} \left( -\nabla F \right) = \mathbf{c}_{j-1} + \alpha \Delta \mathbf{c} \tag{8}$$

**Algorithm 1:** Unconstrained Well Trajectory Optimization
*Input.* An initial vector $\mathbf{c}$, BCB, GCB, NCB
*Output.* $\mathbf{c}^*$ that minimizes the objective.
1. Compute the Newton step: $\Delta \mathbf{c} = -(\nabla^2 \mathrm{F})^{-1} \nabla \mathrm{F}$
2. Determine step size $\alpha$ using a line search.
3. Update $\mathbf{c}$ according to Eq. 8.
4. Stop if $\nabla F^T (\nabla^2 \mathrm{F})^{-1} \nabla \mathrm{F} < \varepsilon$, otherwise repeat from 1.

Initializing $\mathbf{c}$ is straightforward, for example, a horizontal well with an elevation equal to the average BCB could be used. The quantity used for stopping criteria is called the Newton decrement (Boyd and Vandenbergh, 2004), and can be interpreted as the directional derivative of $F$ in the direction of $\Delta \mathbf{c}$.

When the decrement is close to zero, indicated by a small value, $\varepsilon$, a minimum of the objective has been found. Because Algorithm 1 is unconstrained, it will tend to result in trajectories that follow the BCB as close as possible. If large changes in elevation are present in the base, then the trajectory could also have large elevation deviations and this is not necessarily optimal for recovery. Algorithm 1 could be used to optimize the elevation of a horizontal well by zeroing the components of $\nabla F$ and $\nabla^2\mathrm{F}$ associated with endpoint slope and initializing $\mathbf{c}$ to be horizontal.

Incorporating the two constraints mentioned in the previous section, maximum vertical deviation and maximum slope, is accomplished using the interior point Newton method. Constraints are approximated using logarithmic barrier functions (Figure 9). With these constraints, the objective function is expressed as Eq. 9, where $r$ is a scaling parameter, $a_0$, $a_1$, and $d$ are indicated in Figure 4, and $d_{max}$ and $a_{max}$ are the maximum allowable vertical deviation and slope respectively.

$$G = F - \frac{1}{r}\left[\log\left(d_{\max} - d\right) + \log\left(a_{\max} - \left|a_0\right|\right) + \log\left(a_{\max} - \left|a_1\right|\right)\right] \tag{9}$$

To solve the constrained optimization problem using Newton's method, the gradient and Hessian of Eq. 9 are computed. Interior point methods require a feasible starting vector, $\mathbf{c}$, that is, it cannot violate any of the constraints. In the approach developed, the starting point is a horizontal well with an elevation equal to the maximum observed elevation of the BCB across all realizations. For each iteration of Newton's method, $\mathbf{c}$ is updated using Eq. 10, where $\alpha$ is the step size determined using a line search such as the golden section search (Sun and Yuan, 2006).

$$\mathbf{c}_j = \mathbf{c}_{j-1} + \alpha\left(\nabla^2 G\right)^{-1}\left(-\nabla G\right) = \mathbf{c}_{j-1} + \alpha\Delta\mathbf{c} \tag{10}$$

A line search is used to maintain a feasible $\mathbf{c}$ and to prevent divergence as in Algorithm 1. It is possible that the well trajectory that minimizes the loss falls exactly on one of the constraints. The notion of central path is used so that the trajectory gradually approaches one or all of the constraints, since with the interior point method it is difficult to improve on a solution once constraints are encountered exactly. The central path defines the sequence of optimal vectors, $\mathbf{c}^*$, that minimize the objective for increasing values of $r$. Constrained well trajectory optimization is accomplished by Algorithm 2.

**Algorithm 2:** Constrained Well Trajectory Optimization
*Input.* An initial feasible vector $\mathbf{c}$, BCB, GCB, NCB, $r$
*Output.* $\mathbf{c}^*$ that minimizes the objective.
1. Compute $\mathbf{c}_i^*$:
2. Compute the Newton step: $\Delta\mathbf{c} = -(\nabla^2\mathrm{G})^{-1}\nabla\mathrm{G}$
3. Determine step size $\alpha$ using a line search.
4. Update $\mathbf{c}$ according to Eq. 10.
5. Continue from 6. if $\nabla G^T(\nabla^2\mathrm{G})^{-1}\nabla\mathrm{G} < \varepsilon$, otherwise repeat from 2.
6. Update $r_i = \mu r_{i-1}$
7. Stop if $r_i > R$, otherwise repeat from 1.

In Algorithm 2, $i$ is the iteration number for the sequence of solutions, $\mathbf{c}_i^*$, found for each value of $r$. The value $\mu$ is a multiplier that controls the growth rate of $r$. $\mu = 10$ was used in this work. $R$ is typically set to a large number such as $1 \times 10^9$, at which point the logarithmic barriers are nearly exact approximations to the constraints and the resulting solution is at a minimum of the objective function within the feasible region.

In cases where the BCB, GCB and NCB are characterized by high spatial variability, the objective function may have several local minima or plateaus and the solution from Algorithm 1 or 2 may not be the global minimum. To accommodate this possibility, a random restart component is considered in the algorithm. After Step 7, a new feasible initial $\mathbf{c}$ is randomly generated and the algorithm is restarted at Step 1. If after a sufficient number of restarts the minimum is unchanged, $\mathbf{c}^*$ is assumed to be globally optimal.

## Examples

Several examples are used to demonstrate features of the optimization approach including: convergence of bitumen loss; impact of the maximum slope constraint and the maximum vertical deviation constraint; well position for different values of $\theta$; and the impact of multiple realizations. All examples use wells that are 1200 m long. During optimization, wells are scaled to the $[0,1]$ interval as in the previous sections. The first examples use analytical functions for the BCB surface to demonstrate that the algorithm can converge to the exact base when it can be expressed as a Hermite spline. Functions for the BCB include a linear, parabolic, and cubic function defined in Eq. 11. NCB was set to a constant 10 meters and the GCB was set so that the TCB was flat.

$$\begin{aligned} &\text{linear:} && z_{BCB}(u) = 100 \\ &\text{parabolic:} && z_{BCB}(u) = 100 - 20\left(u - 1/2\right)^2 \\ &\text{cubic:} && z_{BCB}(u) = 100 + 20(u - 1/2)^3 \end{aligned} \tag{11}$$

Maximum slope and maximum vertical deviations constraints were set to 4 degrees and 5 meters respectively. Results are shown in Figure 10. In all cases, the bitumen lost is low and the well trajectory falls approximately on the BCB surface. Large jumps in loss on the convergence plots are associated with a random restart step. Performance was best for the cubic surface since the error is lowest. Also, each random restart converged to a similar minimum value. Variation in minima achieved for the parabolic and linear surfaces indicate these problems were more difficult to solve. Although the BCB functions have less variation in these two cases, the optimal solution is more constrained, that is, for the linear surface, the optimal end-point positions are equal and end-point slopes are zero, and for the parabolic surface the optimal end-point positions are equal and end-point slopes are exactly opposite. Detection of such cases is not part of the algorithm leading to some deviation. In addition to this, the loss is non-zero because the BCB surface is piecewise linear and defined by 19 points, which is indicated using a zoomed in portion of the parabolic example in Figure 11.

The maximum vertical deviation constraint is demonstrated using the parabolic BCB example. Deviations ranging from zero to five in increments of one were set as the constraint (Figure 12). For all cases, optimization converges to a well with a vertical deviation nearly equal to the constraint value (Table 1). The algorithm tends to converge faster for cases where the problem is less constrained relative to the geometry of the BCB surface.

**Table 1:** Deviation constraint and resulting trajectory deviation

| Deviation Constraint | Deviation in Trajectory |
|---|---|
| 0 | 0 |
| 1 | 0.9999 |
| 2 | 1.9999 |
| 3 | 2.9999 |
| 4 | 3.9998 |
| 5 | 4.9994 |

The horizontal well case from Figure 12 can be solved more directly without the use of logarithmic barriers. A single iteration of an exact line search algorithm converges to the minimum under the following parameterization: the initial end-point elevations are set to the maximum value of the BCB; the Newton step is set to $\Delta\mathbf{c} = [1 \quad 1 \quad 0 \quad 0]$, and the initial bracket for the line search is from the maximum BCB to the minimum BCB. This approach is used in the DA optimization algorithm presented in the associated paper. It is much faster and provides a useful initial estimate of the DA value for finding a good DA configuration, prior to executing more advanced well optimization strategies.

To demonstrate the effect of different endpoint slope constraints, a somewhat rougher function is used for the BCB. The function is a convex downward parabola augmented by a sin function (Eq. 12).

$$z_{BCB}(u) = 100 + 20(u - 1/2)^2 + \sin(30u) \tag{12}$$

The NCB function was also changed to follow Eq. 13, so that NCB was high where the BCB was low and should cause the well to intersect the base where the NCB is thin.

$$h_{NCB}(u) = 10\left(1 + \sin\left(30(u - \pi/2)\right)\right) \tag{13}$$

Endpoint slope constraints were set to 0.1, 0.3, 0.5, 0.7 and 5 degrees and the maximum vertical deviation constraint was not imposed. For reference, the absolute slope of the parabolic component of Eq. 12 at $u = 0$ is approximately 0.95 degrees. The slope of the steam-oil interface was set to five degrees. As the slope constraint increases, the well trajectories conform better to the BCB (**Figure 13**). Wells also tend to intersect the local highs of the BCB because of the higher quality associated with lows.

The same example is used to demonstrate the effect of the steam-oil interface angle, $\theta$. A maximum slope of 5 degrees is used for five different cases: $\theta = 1, 4, 8, 10, 45$. Intuitively, as the angle decreases, the well is positioned lower in the BCB surface (Figure 14). For large enough angles, the loss for ineffective well segments is large enough that no portion of the well intersects the BCB.

More realistic surfaces are used for an example involving multiple realizations. The maximum slope constraint was set to 4 degrees and maximum vertical deviation constraint to 5 m. The steam-oil interface angle was set to 3 degrees. 10 realizations were considered (Figure 15). Realizations are indicated with light lines while the minimum, mean, and maximum observed values for BCB and NCB are shown with heavy lines. NCB is plotted as BCB + NCB for visualization purposes. For multiple realizations, the loss is computed using Eq. 7 and is the sum of the loss over all realizations. The well trajectory was initialized to a horizontal well with an elevation equal to the maximum elevation of the BCB realizations, which is 115.37 m. Initial and final loss was 57.23 and 16.25 respectively. Had the well been optimized using the expected value of the BCB rather than all realizations simultaneously, the total loss is significantly higher. For example, shifting the optimal trajectory in Figure 15 down 2 m to be closer to the mean BCB surface results in a loss of 50.5.

A few execution times were recorded from the previous examples. Time depends on factors such as grid resolution, number of realizations, and surface complexity. In general, execution time is fast even for a large number of realizations. For the horizontal well case with 10 realizations, optimization takes approximately 7.6 milliseconds per well. For deviated trajectories and 10 realizations, optimization took roughly 313 milliseconds per well, or 41 times longer. This significant increase in time is one reason for maintaining horizontal wells for the DA configuration optimization problem. Timing was done on a 2.8 GHz processor.

## Conclusions

This paper introduced an approach to optimize well trajectories for the SAGD recovery process. The problem was setup in two dimensions assuming that a three dimensional reservoir model could be summarized by surfaces that represent base and top geometry as well as the distribution of recoverable bitumen. The objective function gives a rough estimate of bitumen left behind for a given problem and trajectory. Moreover, optimization can be solved quickly; therefore, the approach is applicable to optimizing drainage area configurations as discussed in Part I of this two paper series. It is also possible to optimize trajectories with multiple realizations. A clear disadvantage of the approach is the simplicity of the problem representation. Geological complexity may not always make it feasible to approximate the reservoir using surfaces and the objective does not account for the physics of the SAGD recovery process. An area of future research is to develop well trajectory optimization for detailed three dimensional models of drainage areas and with physics-based proxy models. The objective function would be calibrated to simulation results and make it possible to consider cumulative oil production and steam-oil ratio during the trajectory optimization process.

## References

Boyd, S., Vandenberghe, L., 2004. Convex optimization. Cambridge University Press, 730

Butler, R.M., 1994. Horizontal wells for the recovery of oil, gas and bitumen. The Petroleum Society of the Canadian Institute of Mining, Metallurgy and Petroleum, Calgary Section, 228

Butler, R.M., 1991. Thermal recovery of oil and bitumen. Prentice Hall, 496

Deutsch, C.V., 2010. Estimation of vertical permeability in the McMurray formation. Journal of Canadian Petroleum Technology, 49(2), 10-18

Deutsch, C.V., 2002. Geostatistical reservoir modeling. Oxford University Press, 384

Doan, L.T., Baird, H., Doan, Q.T., Farouq Ali, S.M., 2003. Performance of the SAGD process in the presence of a water sand – a preliminary investigation. Journal of Canadian Petroleum Technology, 42(1), 25-31

Hearn, D., Baker M.P., 2004. Computer graphics with OpenGL. Pearson Prentice Hall, 880

Law, D.H.-S., Nasr, T.N., Good, W.K., 2003. Field-scale numerical simulation of SAGD process with top-water thief zone. Journal of Canadian Petroleum Technology, 42(8), 32-38

Manchuk, J.G., Deutsch, C.V., 2012. Optimization of drainage area configurations to maximize recovery from SAGD operations. Submitted to Journal of Canadian Petroleum Technology, April 2012

McNamee, J.M., 2007. Numerical methods for roots of polynomials, Part I. Elsevier B. V., 354

Pooladi-darvish, M., Matter, L., 2002. SAGD operation in the presence of overlying gas cap and water layer-effect of shale layers. Journal of Canadian Petroleum Technology, 41(6), 40-51

Ranger, M.J, Gingras, M.K. (2003) Geology of the Athabasca oil sands: field guide & overview. Ranger, M.J., and Gingras, M.K., 123

Scavo, T.R., Thoo, J.B., 1995. On the geometry of Halley's method. The American Mathematical Monthly, 102(5), 417-426

Sun W., Yuan, Y.X., 2006. Optimization theory and methods. Springer Science + Business Media, 699

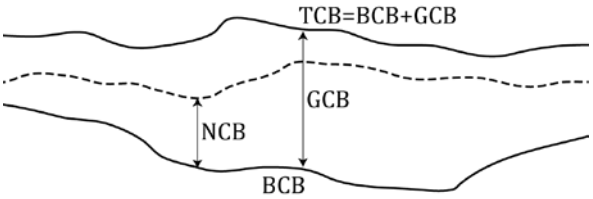


**Figure 1:** Schematic of NCB, BCB and GCB.

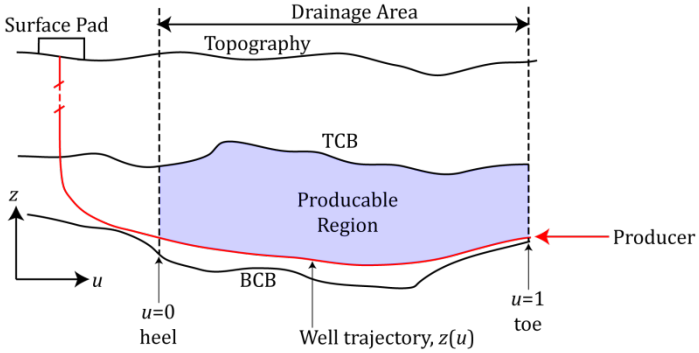


**Figure 2:** Vertical cross section along a production well.

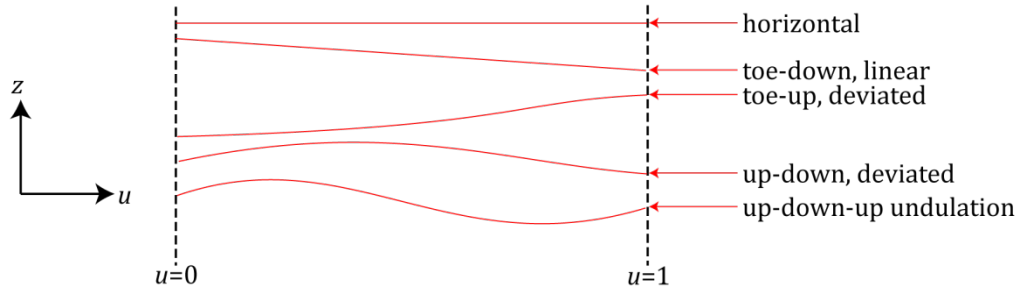


**Figure 3:** Possible well trajectory designs using a Hermite spline.

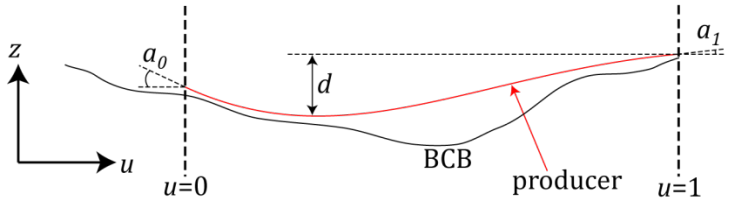


**Figure 4:** Illustration of vertical deviation, $d$, and end-point slopes, $a_0$ and $a_1$.

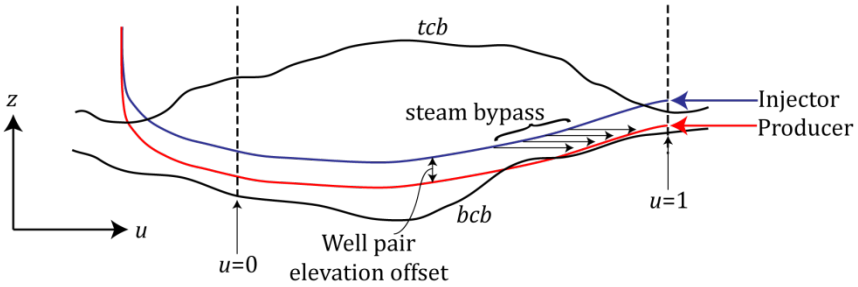


**Figure 5:** Illustration of steam bypass from an injector to a producer in the same well pair.

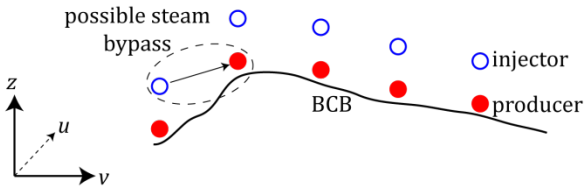


**Figure 6:** Illustration of steam bypass from an injector to a neighbouring producer.

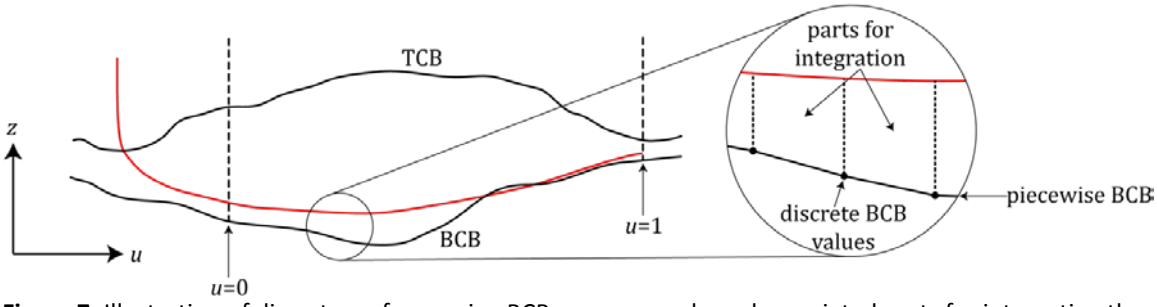


**Figure 7:** Illustration of discrete surfaces using BCB as an example and associated parts for integrating the bitumen lost beneath a producer.

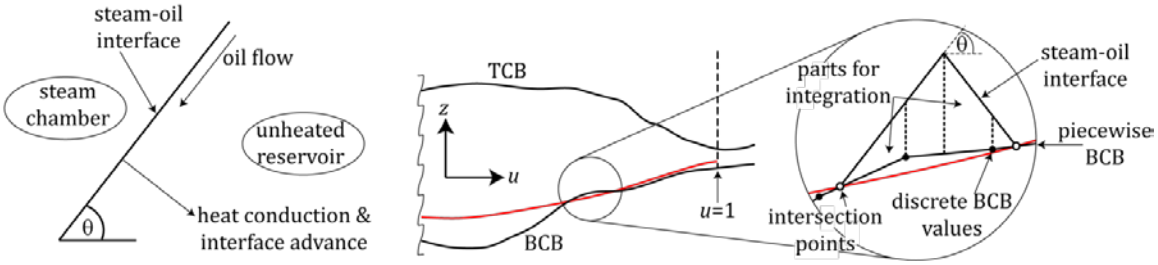


**Figure 8:** Illustration of the steam oil interface as a function of $\theta$ (left) and integration by parts for ineffective segments of a production well (right).

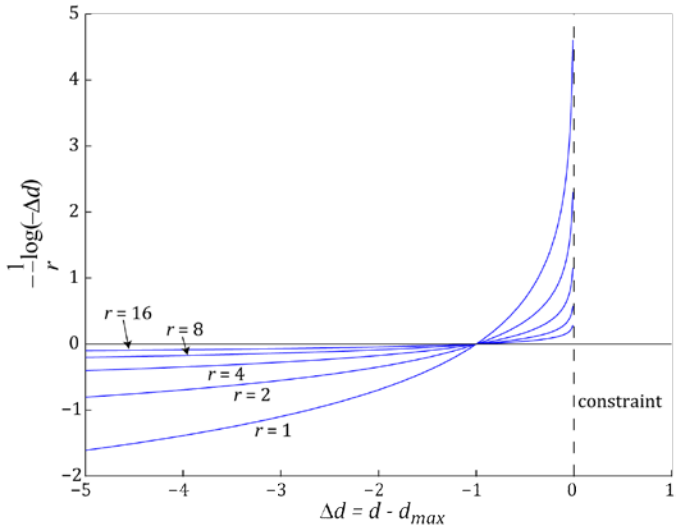


**Figure 9:** Logarithmic barrier for different values of $r$ for the maximum vertical deviation constraint. As $d \rightarrow d_{max}$, the function approaches infinity.

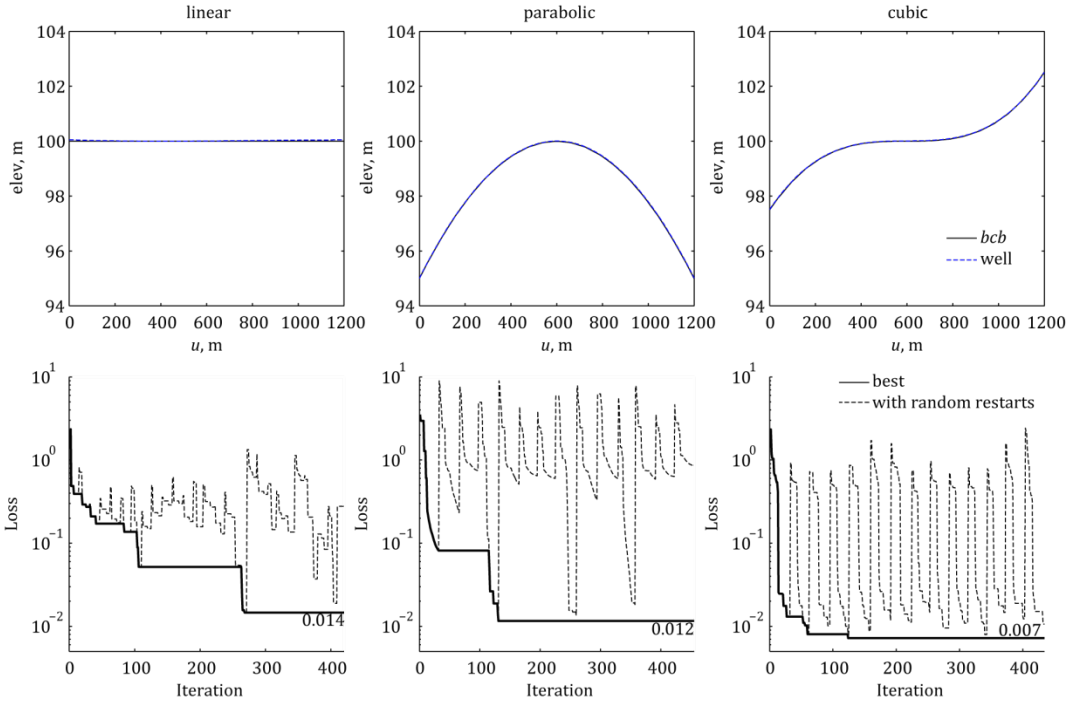


**Figure 10:** Well optimization algorithm applied to three analytical BCB surfaces. Resulting minimum loss is indicated on convergence plots.

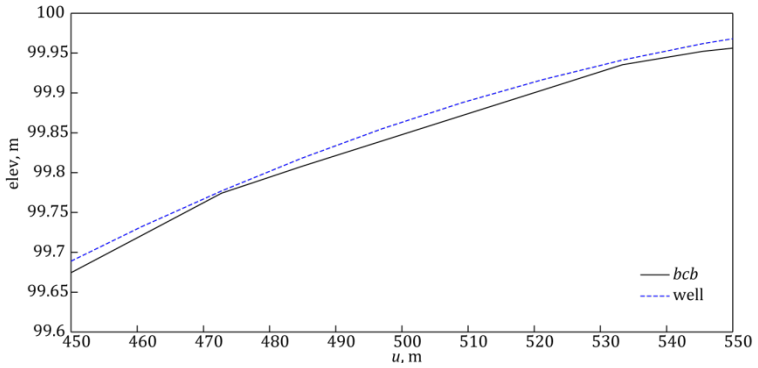


**Figure 11:** Zoomed portion of the parabolic BCB to show piecewise representation.

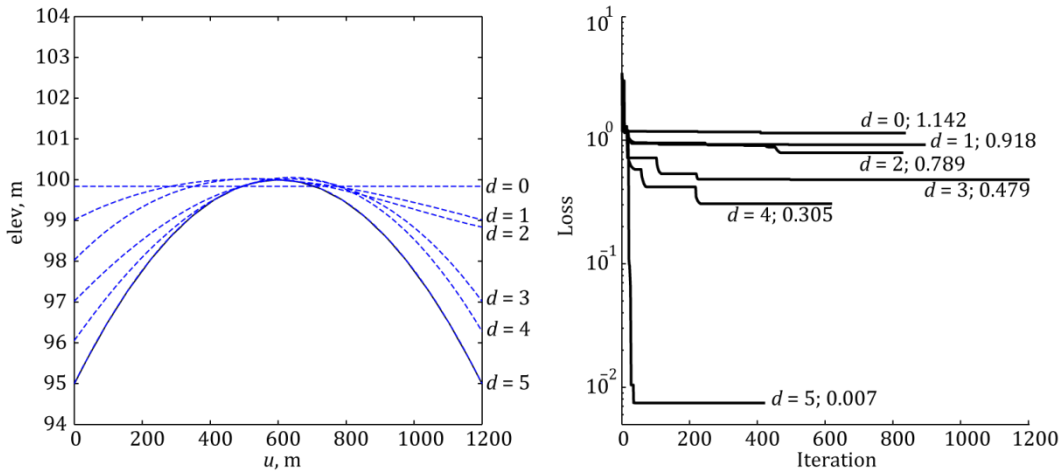


**Figure 12:** Optimized trajectories for various maximum vertical deviations (left) and associated loss convergence curves (right). In right plot, first number is $d$ and second number is minimized loss.

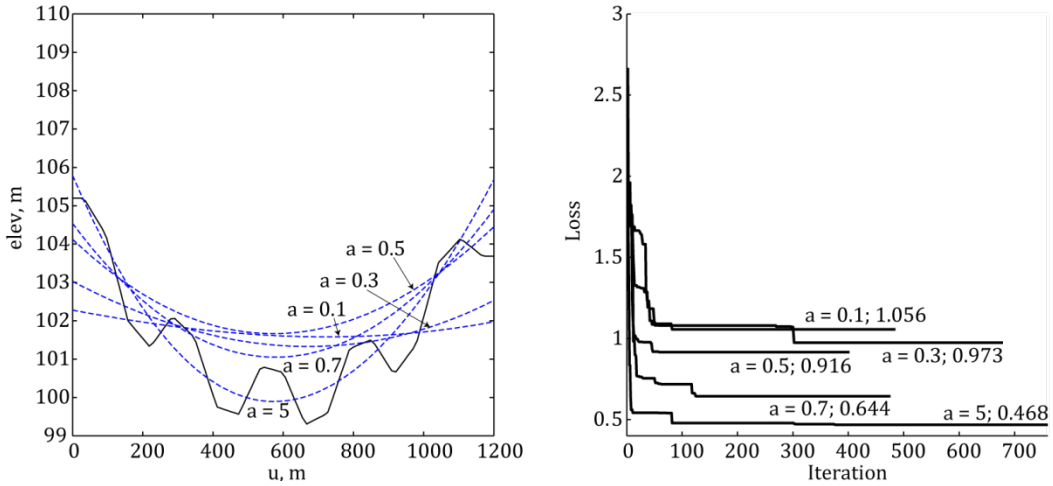


**Figure 13:** Optimized trajectories for various slope constraints (left) and associated loss convergence curves (right). In right plot, first number is $a_{max}$ and second number is minimized loss.

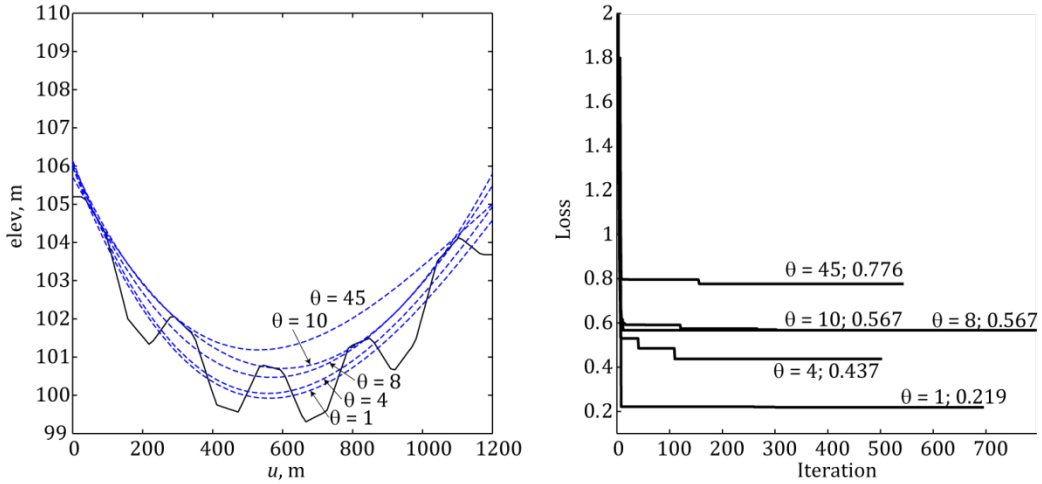


**Figure 14:** Optimized trajectories for various steam-oil interface angles (left) and associated loss convergence curves (right). In right plot, first number is $\theta$ and second number is minimized loss.

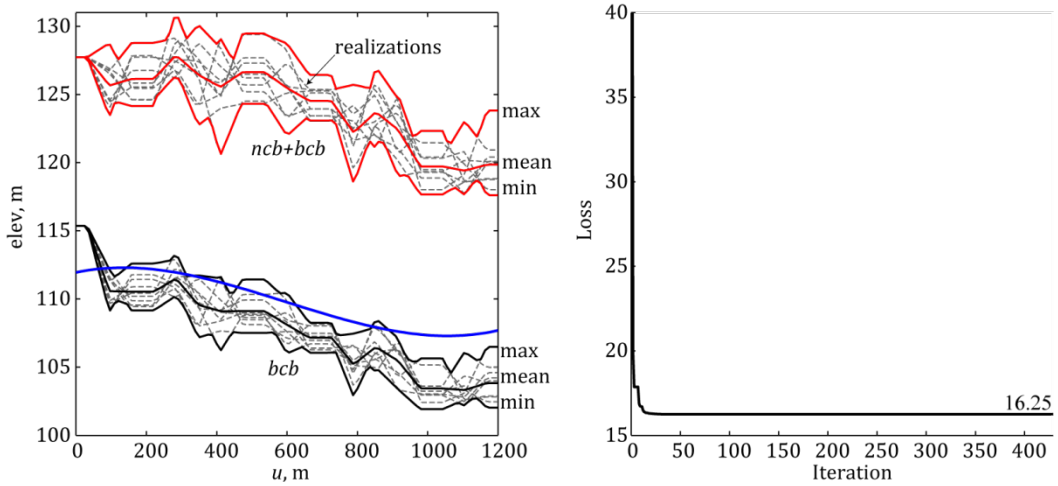


**Figure 15:** Well trajectory optimization with multiple realizations.